



ELSEVIER

Available online at www.sciencedirect.com

SCIENCE @ DIRECT®

Solar Energy Materials
& Solar Cells

Solar Energy Materials & Solar Cells 85 (2005) 1–11

www.elsevier.com/locate/solmat

Light trapping and optical losses in microcrystalline silicon pin solar cells deposited on surface-textured glass/ZnO substrates

J. Springer^{a,b,*}, B. Rech^a, W. Reetz^a, J. Müller^a, M. Vanecek^b

^a*Institute of Photovoltaics, Forschungszentrum Jülich GmbH, Jülich D-52425, Germany*

^b*Institute of Physics, Academy of Sciences of the Czech Republic, Cukrovarnicka 10, Prague 6 CZ-16253, Czech Republic*

Received 23 February 2004; accepted 27 February 2004

Abstract

Influence of front TCO thickness, surface texture and different back reflectors on short-circuit current density and fill factor of thin film silicon solar cells were investigated. For the front TCO studies, we used ZnO layers of different thickness and applied wet chemical etching in diluted HCl. This approach allowed us to adjust ZnO texture and thickness almost independently. Additionally, we used optical modeling to calculate optical absorption losses in every layer. Results show that texture and thickness reduction of front ZnO increase quantum efficiency over the whole spectral range. The major gain is in the red/IR region. However, the higher sheet resistance of the thin ZnO causes a reduction in fill factor. In the back reflector studies, we compared four different back reflectors: ZnO/Ag, Ag, ZnO/Al and Al. ZnO/Ag yielded the best, Al the worst light trapping properties. Furthermore, the Ag back contact turned out to be superior to ZnO/Al for microcrystalline cells. Finally, the smooth ZnO/Ag back contact showed a higher reflectivity than the rough one. We prepared pin cells with rough and smooth ZnO/Ag interface, leaving the roughness of all other interfaces unchanged.

© 2004 Elsevier B.V. All rights reserved.

Keywords: Microcrystalline silicon; Texture-etched zinc oxide; Optical losses; Rough silver back reflector; Optical modeling

*Corresponding author. Institute of Photovoltaics, Forschungszentrum Jülich GmbH, Jülich D-52425, Germany.

E-mail address: springer@fzu.cz (J. Springer).

1. Introduction

In microcrystalline silicon ($\mu\text{c-Si}$) thin film solar cells one desires to minimize the i-layer thickness to reduce deposition time and costs. Consequently, due to the low-absorption coefficient of $\mu\text{c-Si}$ for long wavelength light, light trapping is extremely important. In the pin cell configuration, efficient light trapping is obtained by combining textured transparent conductive oxide (TCO) films as front contact with highly reflective TCO/metal back reflectors (BR). However, due to the multiple passes of scattered light within the solar cell, light absorption is also enhanced in photovoltaically non-active layers like front TCO and TCO/metal back contact. Therefore, spectral response in the infra-red (IR) region will be sensitive to the TCO/metal reflectivity and the front TCO absorption coefficient. On the other hand, the required low sheet resistance of the TCO calls for thicker or more conductive front TCO layers, both usually increase absorption losses. Hence, front TCO type and thickness must be optimized with respect to the competing requirements of good electrical and optical properties. This paper shows the influence of front TCO thickness, texture and back reflector on short-circuit current density j_{SC} and fill factor FF of $\mu\text{c-Si}$ pin solar cells. Such a study was made possible by the use of very homogeneous magnetron sputtered ZnO layers, whose thickness and texture can be adjusted almost independently of the bulk material properties. Additionally to this experimental study, we calculated optical absorption losses in all layers within the solar cell. We use our optical model to study four characteristic solar cells deposited on different glass/ZnO substrates.

2. Experimental

The ZnO films applied as front contacts were prepared by Applied Films on $30 \times 40 \text{ cm}^2$ glass substrates in an in-line DC-magnetron sputtering system from ceramic targets [1]. These highly conductive and transparent layers (Fig. 1) are very homogeneous. Some of these initially smooth films of various thickness (between 500 and 1500 nm) were texture-etched in diluted (0.5%) HCl yielding surfaces with different roughness and light scattering properties [2,3]. The etching rates were between 2 and 5 nm/s. The $1.2 \mu\text{m}$ thick $\mu\text{c-Si:H}$ pin cells were prepared by 13.56 MHz PECVD in a $30 \times 30 \text{ cm}^2$ reactor [4]. This large area reactor allowed us to prepare all $\mu\text{c-Si}$ pin cells presented here on $5 \times 10 \text{ cm}^2$ substrates in one run [5] in a deposition regime of high pressure and high power at an i-layer deposition rate of 5 \AA/s . Only the samples for the polishing experiment (see below) were prepared separately. The resulting cell efficiencies varied between 4% and 8% depending on the front TCO and BR properties. The ZnO/Ag and the Ag back reflectors as well as the ZnO layers for the ZnO/Al back reflectors were RF-magnetron sputtered from ceramic ZnO targets. The aluminum layers were electron-beam evaporated. To study the influence of the ZnO/metal interface roughness, some samples were prepared with a very thick back ZnO (600 nm) which was chemo-mechanically polished in a water-based solution before silver deposition. By this procedure we reached a

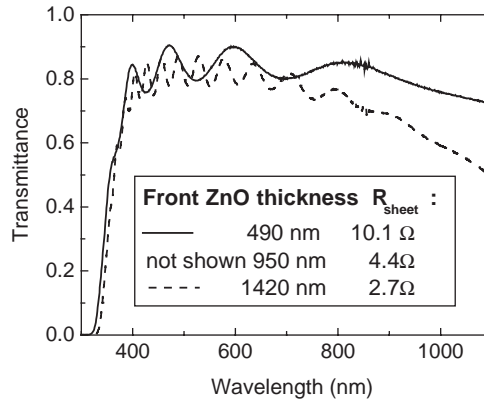


Fig. 1. Transmittance and sheet resistance R_{sheet} of the glass/ZnO substrates before etching (smooth films).

smooth ZnO/Ag interface conserving roughness of all other interfaces. The solar cell area was 1 cm^2 defined by the back contact. All cells were characterized by light I – V measurements under AM1.5 illumination (100 mW/cm^2 , 25°C) and by reverse bias (-0.5 V) quantum efficiency measurements (QE). Furthermore, the total reflectance of the cells and the transmittance of the glass/ZnO layers were determined using a commercial dual beam spectrometer (Lambda 19, Perkin Elmer Co.) with an integrating sphere.

To determine the optical properties of smooth and rough BRs we prepared the following test structures: initially smooth glass/ZnO(600 nm) substrate was texture-etched in diluted HCl. Silver layer (500 nm) and covering ZnO layer (30 nm) were sputtered on this rough substrate yielding rough ZnO/Ag BR. Smooth BR was prepared similarly, we just skipped the texture-etching step. Samples were characterized from ZnO(30 nm)/Ag side. Resulting rms roughnesses are 106 and 14 nm, respectively. The absorptances of rough and smooth BRs were measured by Photothermal Deflection Spectroscopy. Experimental details can be found in Ref. [6].

We used our optical model [7–9] to calculate absorption losses in all layers within the solar cell. This model uses scalar scattering theory [10] and allows modeling of multilayer structures with nano-rough interfaces.

3. Results and discussion

3.1. Front TCO study

To demonstrate the etching (texturing) effect, we prepared two cells with ZnO/Ag BR. For these cells the “standard” ZnO/Ag BR with ZnO thickness of $\approx 100 \text{ nm}$ was applied. One cell was deposited on the smooth 500 nm ZnO substrate without etching (Fig. 2a). The second one was prepared on another piece of this ZnO/glass

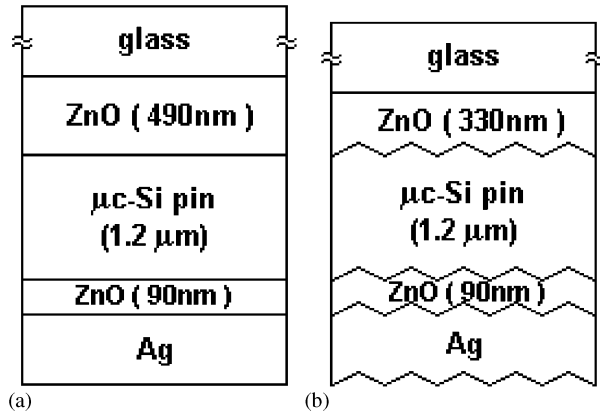


Fig. 2. Two schematic layer structure of $\mu\text{c-Si:H}$ pin cells with ZnO/Ag back reflector co-deposited on smooth, non-etched (a) and texture-etched (b) glass/ZnO substrates.

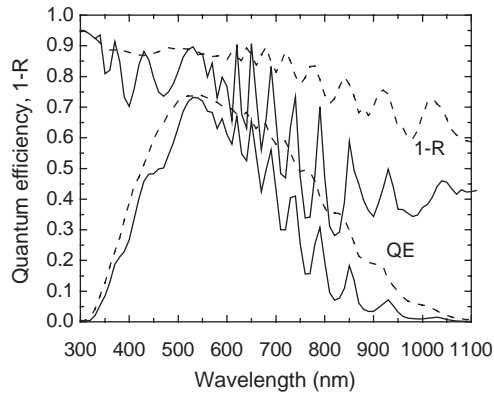


Fig. 3. Quantum efficiency QE and (1- R) curves measured for $\mu\text{c-Si}$ pin solar cells on the thin texture-etched (dashed lines) and smooth (solid) ZnO coated glass. The corresponding short-circuit densities are 19.1 and 14.3 mA/cm^2 , respectively, (R =total reflectance).

substrate which was etched for 30 s to obtain a textured surface (Fig. 2b). Here the resulting ZnO thickness was 330 nm. Fig. 3 shows the QE of these two cells as well as the (1- R) curves. The difference between the (1- R) and QE curves is a measure for the optical absorption losses in glass/ZnO substrate, back reflector and photovoltaically non-active Si layers (p^+ , n^+) supposing that all photoexcited charge carriers generated in the $\langle i \rangle$ $\mu\text{c-Si}$ are collected.

To learn more about the ZnO losses, we used ZnO of three different initial thickness to obtain a front ZnO thickness series of 330, 870 and 1370 nm after 30 s of etching. The thick substrate has a higher conductivity, which increases FF due to the

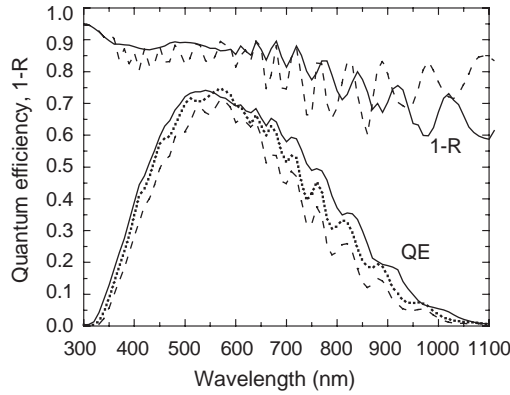


Fig. 4. Measured quantum efficiency QE and (1-R) for the front ZnO thickness series: 330 nm (full line; 19.1 mA/cm², FF = 68%), 870 nm (dots; 17.6 mA/cm², FF = 72%) and 1370 nm (dashed; 15.5 mA/cm², FF = 75%).

reduced series resistance losses. However, lower optical transparency of the thick substrate leads to lower QE and j_{SC} (Fig. 4).

We calculated the optical absorption losses for the four cells described above. The results are plotted in Fig. 5 showing the losses in each layer. The corresponding modeling parameters are shown in Table 1. All other parameters are kept same for all the four analyzed cells: 40 nm n⁺, 90 nm back ZnO, experimentally determined reflectance at rough ZnO/Ag interface (see below). Thickness of the layers (except doped p⁺, n⁺) were close to the measured values, the main criteria being the exact position of interference fringes. The thickness of the doped p⁺ layers could not be measured on the textured ZnO films and was fitted with the help of the model. The rather thick n⁺ layer was not optimized for maximum efficiency. The optical properties of all layers were experimentally determined [6–8, 10, 11].

Both experimental results (Fig. 3) and our model (Fig. 5a,b) show that the etching increases QE over the whole spectral range, and at the same time reflection decreases. In the short-wavelength region (<550 nm) this is due the anti-reflection effect introduced by the rough interface [12]. In the red/IR region the etching introduces light scattering and consequently light trapping. The scattering reduces the coherent part of the light and leads to a smoothing of the interference fringes. In our experiment the fringes are weak but still visible even for the textured ZnO. It shows that a part of the light is not scattered. Additionally, our model shows that etching increases absorptance in all layers (Table 2). For short wavelengths the main absorption losses are in p⁺. Absorption losses in front ZnO are dominant for the red/IR ($\lambda > 600$ nm) due to the free carrier absorption. Comparing the thin and the thick ZnO substrate (Figs. 4 or 5b,d), optical losses are mostly in this region. This is enhanced by multiple passes of scattered light within the solar cell (compare the cells with and without light trapping in Figs. 3 or 5a,b)). Smaller losses are observed in the short wavelengths ($\lambda < 600$ nm). The lower transparency of the thick ZnO partly

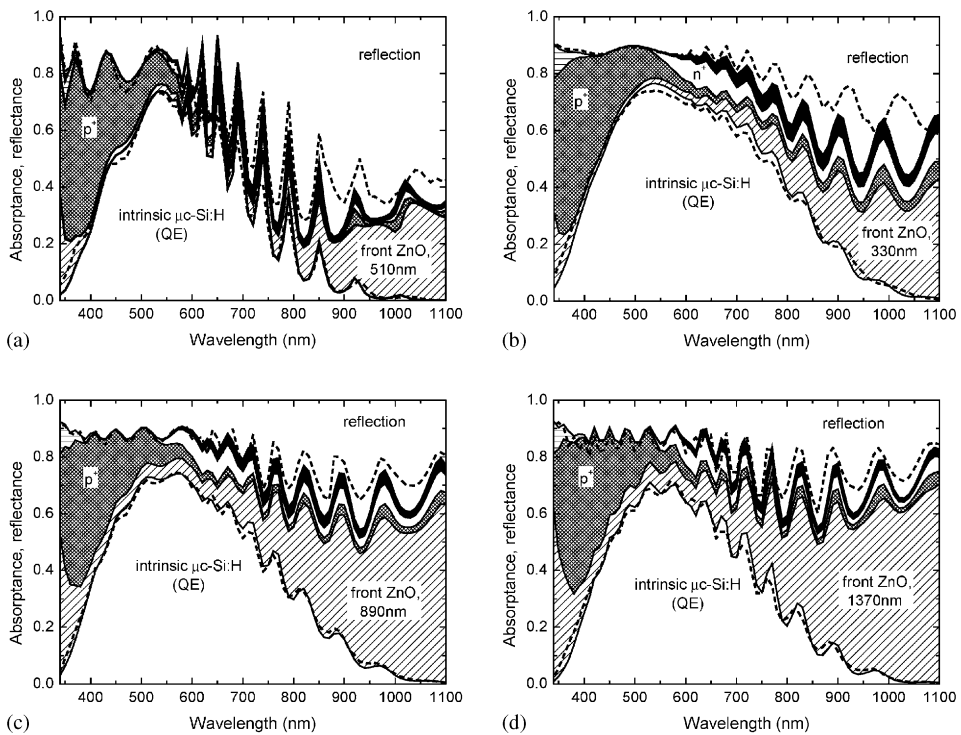


Fig. 5. Measured (dashed lines) and calculated (solid) QE and $(1-R)$. The area between QE and $(1-R)$ corresponds to the absorption losses in front ZnO, p^+ , n^+ , silver (black) and glass + back ZnO (horizontal lines). The calculations are results of our optical model and the calculated QEs equal to absorbances in the $\langle i \rangle$ $\mu\text{c-Si}$ layers.

Table 1

Parameters used in the optical model to calculate optical losses in samples (a)–(d)

Sample	Description	rms roughness (nm)	Thickness (nm)		
			Front ZnO	p^+	$\langle i \rangle$ $\mu\text{c-Si:H}$
(a)	thin ZnO, no etching	5	510 (490 ± 20)	40	1190 (1150 ± 100)
(b)	thin ZnO, 30 s etched	35	330 (330 ± 30)	25	1170 (1150 ± 100)
(c)	mid ZnO, 30 s etched	25	890 (870 ± 40)	25	1155 (1150 ± 100)
(d)	thick ZnO, 30 s etched	23	1370 (1420 ± 60)	35	1150 (1150 ± 100)

The parameters are close to measured values (in brackets). The thick textured ZnO film has a lower rms roughness than the thin one.

explains the QE decrease in this region. However, the losses are probably also connected to less efficient texturing of the thick ZnO (see the rms roughness in Table 1) leading to reduced scattering and also to a reduced anti-reflection effect.

Table 2

Short-circuit current density J_{sc} and optical losses calculated for samples (a)–(d)

	ZnO thickness rms roughness	j_{sc} (mA/cm ²)	Optical losses (mA/cm ²)					
			R	ZnO	p ⁺	n ⁺	ZnO _{back}	Ag
(a)	510 nm, 5 nm	14.7	19.0	5.0	3.5	1.0	0.04	0.65
(b)	330 nm, 35 nm	19.5	11.3	5.5	3.7	2.2	0.13	1.45
(c)	890 nm, 30 nm	17.8	9.7	10.3	3.2	1.8	0.10	1.11
(d)	1370 nm, 23 nm	15.7	9.6	12.3	3.6	1.5	0.07	0.88

The losses are quantified in mA/cm². In case of no optical losses, 44 mA/cm² is the theoretical limit for j_{sc} (given by the 100 mW AM1.5).

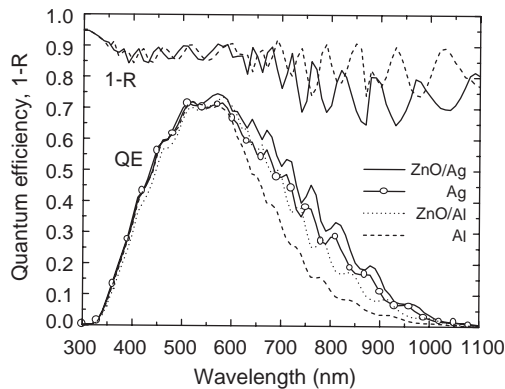


Fig. 6. Quantum efficiency QE and (1-R) measured for different back reflectors, (R =total reflectance).

3.2. Back reflector study

3.2.1. Different types of back reflector

The 870 nm thick ZnO (after 30 s of etching) was applied for μ c-Si cells with four different back reflectors: ZnO/Ag, Ag, ZnO/Al and Al. As expected, the best cell is obtained with the ZnO/Ag BR, the worst (5 mA/cm² reduction in j_{sc}) with the Al BR (Fig. 6). No difference in QE for wavelengths < 600 nm was observed because in this spectral region the QE is sensitive only to the front ZnO and p- and i-layer properties, thus nicely demonstrating the homogeneity of ZnO and Si deposition.

An interesting result is that the Ag BR yields a higher current than the ZnO/Al BR. In previous experiments with a-Si pin solar cells both BRs showed a similar effect on cell performance. Table 3 helps with the explanation. For a-Si cells, good reflectivity is important in the region between 550 and 750 nm. The reflectance at 600 nm (which we take as a measure) is very similar for Ag and ZnO/Al. On the other hand, for microcrystalline silicon cells good reflectivity of the BR is essential in the

Table 3

Experimentally determined current loss Δj_{sc} of different types of back reflectors BR compared to the ZnO/Ag BR and the calculated internal reflectance for the a-Si/BR structure at 600 nm and the μ c-Si/BR structure at 800 nm

BR	Measured Δj_{sc} (mA/cm ²)	Calculated	
		$R_{600\text{ nm}}$	$R_{800\text{ nm}}$
ZnO/Ag	−0.0	0.94	0.96
Ag	−1.0	0.87	0.94
ZnO/Al	−2.6	0.85	0.77
Al	−4.7	0.70	0.65

whole region 600–1100 nm. An aluminum interband absorption occurs within this region (at $\lambda \approx 800$ nm) [13] which causes enhanced absorption in the Al and hence low reflectivity for the ZnO/Al BR. Note that all calculations in Table 3 are made assuming smooth interfaces (simple Fresnel's equations). The used optical constants of Ag and Al can be found in Ref. [13], for μ c-Si and a-Si in Refs. [7, 10, 11]. For the ZnO we applied values $n_{600\text{ nm}} = n_{800\text{ nm}} = 2.0$, $k = 0$ which were estimated from the transmittance/reflectance measurements of a 1 μ m thick smooth back ZnO layer on a glass substrate. We are aware that the material parameters in our cells might deviate from the used literature data (see below). However, losses due to the aluminium interband absorption around $\lambda = 800$ nm remain the dominant effect.

3.2.2. Reflectivity of rough ZnO/Ag back reflector

For the reflectance calculation in Table 3 we used literature data and applied Fresnel's equations, which are valid only for smooth interfaces. It is well known that a rough metal interface (such as our metal back contacts) has lower total reflectance than a smooth one [14–17].

We did two experiments to study this effect and its influence on the solar cell. First we measured the reflectivity R of smooth and rough ZnO/Ag interfaces by Photothermal Deflection Spectroscopy [18]. This method allows us to reach a higher precision than by standard spectrometer measurement. The experiment is described in Ref. [6]. In the IR region our rough ZnO/Ag interface has 2–3 \times higher absorptance A ($A = 1 - R$) than the smooth one (Fig. 7). This value will depend on the surface topography and also quality of the ZnO/Ag BR. However, the general trend should be always visible.

In the second experiment we studied this effect directly in our solar cells by smoothing the back ZnO before Ag deposition, while the roughness of all other interfaces was conserved (Fig. 8). We compared this cell to a non-polished cell with the standard rough ZnO/Ag BR (Fig. 9). Special attention was paid to prepare the polished and the non-polished cells with similar final back ZnO thickness of ≈ 350 nm.

The polishing reduces scattering and consequently also light trapping. Total reflectance increases and the interference fringes are more pronounced. Absorption

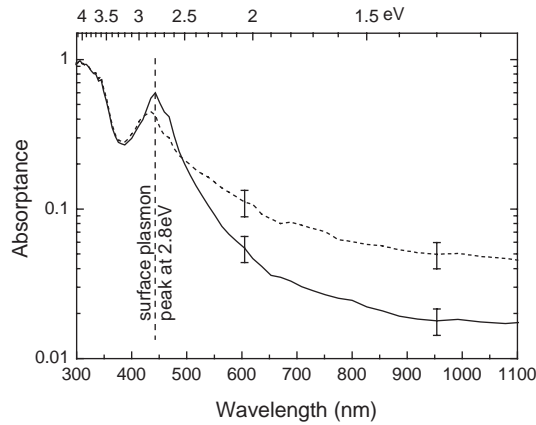


Fig. 7. Absorbance of smooth (solid line) and rough (dashed) ZnO/Ag back reflector measured by photothermal deflection spectroscopy.

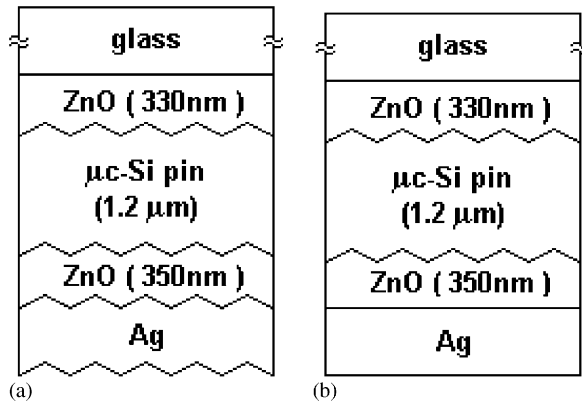


Fig. 8. Schematic sketch of two $\mu\text{c-Si}$ pin cells for back reflector study, with non-polished (rough) (a) and polished (smooth) (b) ZnO/Ag interface.

in non-active layers (mostly in front ZnO and BR), described by $(1-R-QE)$, decreases due to a less efficient light trapping and a higher ZnO/Ag reflectivity. However, one can observe very similar QE and j_{SC} , so the negative effect of reduced light trapping is almost balanced by the advantage of the higher ZnO/Ag reflectivity. From the latter, one can predict advantages of the smooth metal back contact. If it is possible to realize a front TCO that yields almost 100% of optical scattering up to $\lambda \approx 1000 \text{ nm}$ in the front part of the cell, a smooth ZnO/metal BR should improve j_{SC} .

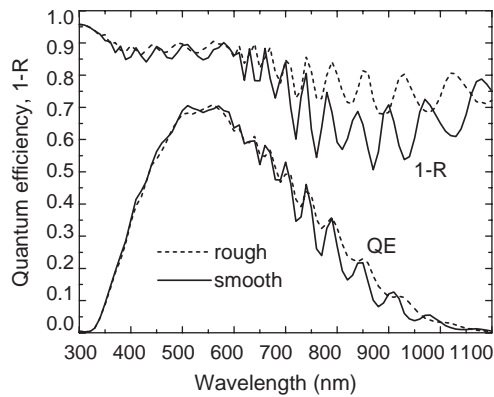


Fig. 9. Quantum efficiency QE and (1-R) for cells with rough and smooth ZnO/Ag interfaces. The short-circuit current densities were 16.4 and 16.0 mA/cm², respectively, (R = total reflectance).

4. Conclusions

Texture-etching of the front ZnO increases quantum efficiency over the whole spectral range. This is partly due to an anti-reflection effect in the blue/UV wavelength region and mostly due to an enhanced light trapping in the red/IR. On other hand better light trapping increases optical absorption in all layers within solar cell. A further improvement in short-circuit current density can be easily achieved by using a thinner front ZnO, which reduces free carrier absorption losses in the red/IR as well as absorption around optical edge of ZnO in the blue/UV region. However, the thinner front ZnO is connected to higher ZnO sheet resistance and hence lower fill factor due to enhanced electrical losses. To avoid these losses and maintain low optical absorption, ZnO films with high electron mobility are required.

We further experimentally compared microcrystalline pin cells with ZnO/Ag, Ag, ZnO/Al and Al back reflectors. As expected, ZnO/Ag is the best and Al is the worst one. Interestingly, the cell with the ZnO/Al back reflector shows lower performance than with Ag back reflector. The low reflectivity of aluminium due to interband absorption at around $\lambda = 800$ nm, a wavelength region very important for μ c-Si cells, explains this observation.

Finally, we demonstrated the advantage of a smooth back contact, which has higher reflectivity than the standardly used rough one. In our cell, this advantage was balanced by losses arising from less efficient light scattering. However, for a highly diffusive front ZnO, scattering at the back contact should be less important and the higher reflectivity should increase quantum efficiency in the red/IR region.

Acknowledgements

The authors thank M. Ruske from Applied Films GmbH, Alzenau, Germany for supplying glass/ZnO substrates, J. Frystacký from Optics department, IP Prague for

polishing of ZnO, W. Appenzeller and G. Schöpe from IPV FZ Jülich for extensive technical assistance and S. Michel from IPV FZ Jülich for the evaporation.

This work was supported by the Bundesministerium für Wirtschaft (BMWi) under contract no. 0329854A and by the European Commission (contract: ENK6-CT-2000-00321).

References

- [1] J. Müller, G. Schöpe, O. Kluth, B. Rech, M. Ruske, J. Trube, B. Szyszka, X. Jiang, G. Bräuer, *Thin Solid Films* 392 (2001) 327.
- [2] O. Kluth, A. Löffl, S. Wieder, C. Beneking, W. Appenzeller, L. Houben, B. Rech, H. Wagner, S. Hoffmann, R. Waser, J.A. Anna Selvan, H. Keppner, *Proceedings of the 26th IEEE PVSC, Anaheim, USA, 1997*, p. 715.
- [3] B. Rech, O. Kluth, T. Repmann, T. Roschek, J. Springer, J. Müller, F. Finger, H. Stiebig, H. Wagner, *Sol. Energy Mater. Sol. Cells* 74 (2002) 439.
- [4] T. Repmann, W. Appenzeller, T. Roschek, B. Rech, O. Kluth, J. Müller, W. Psyk, R. Geyer, P. Lechner, *Proceedings of the 17th EC-PVSEC, Munich, Germany, 2001*, p. 2836.
- [5] B. Rech, T. Roschek, T. Repmann, J. Müller, R. Schmitz, W. Appenzeller, *Thin Solid Films* 472 (2003) 157.
- [6] J. Springer, A. Poruba, L. Müllerova, M. Vanecek, O. Kluth, B. Rech, *J. Appl. Phys.* 95 (2004) 1427.
- [7] J. Springer, A. Poruba, A. Fejfar, M. Vanecek, L. Feitknecht, N. Wyrsh, J. Meier, A. Shah, *Proceedings of the 16th EC-PVSEC, Glasgow, UK, 2000*, p. 434.
- [8] J. Springer, A. Poruba, M. Vanecek, S. Fay, L. Feitknecht, N. Wyrsh, J. Meier, A. Shah, T. Repmann, O. Kluth, H. Stiebig, B. Rech, *Proceedings of the 17th EC-PVSEC, Munich, Germany, 2001*, p. 2830.
- [9] M. Vanecek, J. Springer, A. Poruba, O. Kluth, T. Repmann, B. Rech, N. Wyrsh, J. Meier, A. Shah, *Proc. WCPEC-3, Osaka, Japan, 2003*, p. 1527.
- [10] A. Poruba, A. Fejfar, Z. Remes, J. Springer, M. Vanecek, J. Kocka, J. Meier, P. Torres, A. Shah, *J. Appl. Phys.* 88 (2000) 148.
- [11] M. Vanecek, A. Poruba, in: M.F. Thorpe, L. Tichy (Eds.), *Properties and Application of Amorphous Materials*, Kluwer Academic Publications, Dordrecht, 2001, p. 401.
- [12] W. Frammelsberger, R. Geyer, P. Lechner, H. Rübel, H. Schade, J. Müller, G. Schöpe, O. Kluth, B. Rech, *Proceedings of the 16th EC-PVSEC, Glasgow, UK, 2000*, p. 389.
- [13] E.D. Palik, *Handbook of Optical Constants of Solids*, Academic Press, New York, 1985, p. 350 & 369.
- [14] D. Beaglehole, O. Hunderi, *Phys. Rev. B* 2 (1970) 309.
- [15] H. Raether, in: G. Hohler (Ed.), *Springer Tracts in Modern Physics, Vol. 111, Surface Plasmons on Smooth and Rough Surfaces and on Gratings*, Springer, Berlin, 1988.
- [16] G. Harbeke, in: G. Harbeke (Ed.), *Polycrystalline Semiconductors*, Springer, Berlin, 1985, p. 156.
- [17] E. Fontana, R.H. Pantell, *Phys. Rev. B* 37 (1988) 3164.
- [18] N.M. Amer, W.B. Jackson, in: J.I. Pankove (Ed.), *Semiconductors and Semimetals, Vol. 21, part B, Hydrogenated Amorphous Silicon*, Academic Press, Orlando, 1984, p. 83.